CHEMISTRY
A EUROPEAN JOURNAL

DOI: 10.1002/chem.200600213

Relationship between Incoherent Excitation Energy Migration Processes and Molecular Structures in Zinc(II) Porphyrin Dendrimers

Sung Cho,[a] Wei-Shi Li,[b] Min-Chul Yoon,[a] Tae Kyu Ahn,[a] Dong-Lin Jiang,[b] Jiwon Kim,[c] Takuzo Aida,*[b] and Dongho Kim*[a]

Abstract: Multiporphyrin dendrimers are among the most promising architectures to mimic the oxygenic light-harvesting complex because of their structural similarities and synthetic convenience. The overall geometries of dendrimers are determined by the core structure, the type of dendron, and the number of generations of interior repeating units. The rigid core and bulky volume of exterior porphyrin units in multiporphyrin dendrimers give rise to well-ordered three-dimensional structures. As the number of generations of interior repeating units increases, however, the overall structures of dendrimers become disordered and randomized due to the flexibility of the repeating units. To reveal the relationship between molecular structure and processes of excitation-energy migration in multiporphyrin dendrimers, we calculated the molecular structure and measured the time-resolved transient absorption and fluorescence anisotropy decays for various hexaarylbenzene-anchored polyester zinc(II) porphyrin dendrimers along with three types of porphyrin dendrons as references. We found that the congested two-branched type dendrimers exhibit more efficient energy migration processes than one- or three-branched type dendrimers because of multiple energy migration pathways, and the three-dimensional packing efficiency of dendrimers strongly depends on the type of dendrons.

Keywords: dendrimers · energy migration · photophysics · porphyrins · time-resolved spectroscopy

Introduction

Oxygenic photosynthesis performed by plants, green algae, and cyanobacteria is a major process in the conversion of light energy from the Sun to chemical energy that can be used by biological systems.[1–3] Each step of energy transfer in the light-harvesting complex is very fast, and this leads to high energy-conversion efficiency. In this context, there have been tremendous efforts to mimic the natural photosynthetic system for the realization of highly efficient molecular photonic devices such as molecular wires, switches, transistors, and artificial light-harvesting devices.[4–11] The 96 chlorophyll units in cyanobacterial photosystem I (PSI) are congested and three-dimensionally arranged in a protein matrix.[1] Compared with the well-ordered anoxygenic photosynthetic light-harvesting complex, it is unclear why the disordered and randomly oriented geometry of oxygenic PSI was chosen by nature. However, the tightly packed three-dimensional geometry of oxygenic PSI is expected to have the advantage of enormous absorbing capacity. In addition, the relatively short distance between the constituent chlorophyll units gives rise to multiple energy-migration paths to the reaction center to enhance the quantum efficiency of energy transfer.

As one of the strategies in the preparation of artificial light-harvesting systems, multiporphyrin dendrimers have been envisaged,[8,9,12,13] because the properties of dendrimers can be controlled by the core structure, the type of branch, and the generation number. Moreover, due to structural similarities, multiporphyrin dendrimers can be a good approach to mimicking the oxygenic light-harvesting complex

[a] S. Cho, M.-C. Yoon, Dr. T. K. Ahn, Prof. D. Kim
National Creative Research Initiatives Center for Ultrafast Optical Characteristics Control and
Department of Chemistry, Yonsei University, Seoul 120-749 (Korea)
Fax:(+82) 2-2123-2434
E-mail: dongho@yonsei.ac.kr

[b] Dr. W.-S. Li, Dr. D.-L. Jiang, Prof. T. Aida
Aida Nanospace Project
Exploratory Research for Advanced Technology (ERATO)
Japan Science and Technology Agency (JST)
2-41 Aomi, Koto-ku, Tokyo 135-0064 (Japan)
Fax:(+81) 3-5841-7310
E-mail: aida@macro.t.u-tokyo.ac.jp

[c] J. Kim
School of Chemistry, Seoul National University, Seoul 151–747 (Korea)

Supporting information for this article is available on the WWW under http://www.chemeurj.org/ or from the author.

of cyanobacteria, which greatly differs from the two-dimensional cyclic arrangements of LH1 and LH2 complexes in anoxygenic photosynthetic bacteria. Larsen et al. studied energy-migration processes and conformational dynamics in flexible porphyrin dendrimers.[9b] However, quantitative investigations on excitation energy transfer (EET) processes in porphyrin dendrimers have been rather limited, mainly due to the difficulties in molecular modeling caused by their large molecular sizes and various conformers.

To elucidate the structure–property relationship between the dendritic structures and the EET processes occurring in three-dimensional zinc(II) porphyrin dendrimers (Scheme 1), hexaarylbenzene-anchored polyester zinc(II) porphyrin dendrimers and their constituent one-, two-, and three-branched type dendrons were synthesized[14] and studied by time-resolved transient absorption and fluorescence anisotropy measurements.

Results

Steady-state absorption and fluorescence spectra: The absorption spectra of the series of zinc(II) porphyrin dendrimers and dendrons in THF (Figure 1a) are nearly identical and clearly demonstrate weak interchromophore interactions between neighboring porphyrin units. As the number of porphyrin units in the dendrimers increases, the molar extinction coefficients of the Q-bands linearly increase (inset to Figure 1), that is, the light-absorbing capability is proportional to the number of porphyrin units. The dendrimers exhibit slightly blue-shifted and broad B bands at 414 nm, probably due to cofacial geometry and various conformational structures. On the other hand, the spectral shape of the Q-bands remains relatively unchanged as the number of porphyrins in the dendrimers increases due to small transition dipole moments of S_1 states. The nearly identical steady-state fluorescence spectra (Figure 1b) of the dendrimers and dendrons as well as similar fluorescence quantum yields suggest that each porphyrin moiety acts as an individual emitter. To obtain information on the relative orientation between the absorption and emission dipoles of constituent porphyrin units in the dendrimers, their steady-state fluorescence excitation anisotropy spectra in THF were recorded. The anisotropy value generally increases as the molecular volume increases due to slower rotational diffusion motion in solution. However, the anisotropy values become saturated at 0.1, mainly because of the competition between slower rotational diffusion motion and faster energy-migration processes. Therefore, we could expect efficient energy-migration processes in zinc(II) porphyrin dendrimers.

Time-resolved fluorescence decays: Time-resolved isotropic (magic-angle) spontaneous fluorescence decays of zinc(II) porphyrin dendrimers and dendrons in THF were measured by photoexcitation at 405 nm and detection at 450 and 650 nm, respectively (Figure 2). The S_2 state fluorescence decay rates of one- and two-branched type dendrons (**1P$_{Zn}$** and **2P$_{Zn}$**) and dendrimers (**6P$_{Zn}$W**, **12P$_{Zn}$W**, and **24P$_{Zn}$W**) become accelerated as the number of porphyrin units increases. The decay of the S_2 state of zinc(II) porphyrin is mainly due to internal conversion from the S_2 to the S_1 state. As porphyrin molecules interact strongly in porphyrin assemblies, the low-energy exciton-split S_2 state provides a ladder for deactivation processes of the S_2 state. As a consequence, as the molecular interactions become stronger in porphyrin arrays, decay of the the S_2 state becomes accelerated. On the other hand, the S_2 state fluorescence decay rate of **3P$_{Zn}$** is already fast, similar to that of **12P$_{Zn}$W**, that is, the zinc(II) porphyrin units in **3P$_{Zn}$** strongly interact with each other. In addition, the fluorescence decay rates of three-branched type dendrimers such as **18P$_{Zn}$W** and **36P$_{Zn}$W** are easily saturated compared with those of two-branched type dendrimers **12P$_{Zn}$W** and **24P$_{Zn}$W**, and this implies that the packing efficiency is similar in both **18P$_{Zn}$W** and **36P$_{Zn}$W** and the interactions among the zinc(II) porphyrin units in **3P$_{Zn}$** play a major role in the acceleration of the S_2 state fluorescence decays in **18P$_{Zn}$W** and **36P$_{Zn}$W**.

The S_1 state lifetimes of one-, two-, and three-branched type dendrons (**1P$_{Zn}$**, **2P$_{Zn}$** and **3P$_{Zn}$**) are similar (Figure 2b) and Table 1). On the other hand, zinc(II) porphyrin dendrimers constituted of three types of dendrons exhibit decreased fluorescence lifetimes in the order of one-, three-, and two-branched type dendrimers. Since the transition dipole moments of S_1 states of porphyrins are much smaller than those of S_2 states, the S_1 state lifetimes of zinc(II) porphyrin dendrimers are sensitive to molecular structural parameters such as interchromophore distance and relative orientation. In addition, the relatively long S_1 state lifetimes for the Q states of porphyrins compared with the short-lived S_2 states provide more chances for molecular motions to be involved in the nonradiative decay channels for the S_1 state such as excimer formation. In other words, well-arranged dendrimers with rigid architectures are expected to have longer S_1 state lifetimes. Accordingly, one-branched type dendrimer **6P$_{Zn}$W** having an ideal in-plane circular arrangement with relatively long interchromophore distance has a longer S_1 state lifetime. Three-branched type dendrimers such as **18P$_{Zn}$W** and **36P$_{Zn}$W** exhibit a slight reduction in the S_1 state lifetimes compared with their building block **3P$_{Zn}$**, that is, these dendrimers form compact three-dimensional architectures with three-branched type dendrons as building blocks. On the other hand, conformational flexibility seems to exist in two-branched type dendrimers such as **12P$_{Zn}$W** and **24P$_{Zn}$W** to provide nonradiative decay channels including excimer formation. This feature presumably leads to shorter S_1 state lifetimes, because two-branched building block **2P$_{Zn}$** has enough space for excimer formation induced by a short interchromophore distance through the rigid core. Especially **12P$_{Zn}$W** exhibits enhanced fluorescence emission at a relatively long wavelength of 700 nm and an increased long-lived component in the fluorescence decay suggesting excimer formation (Figures 1b and 2b). The similar fluorescence quantum yields of zinc(II) porphyrin dendrimers to

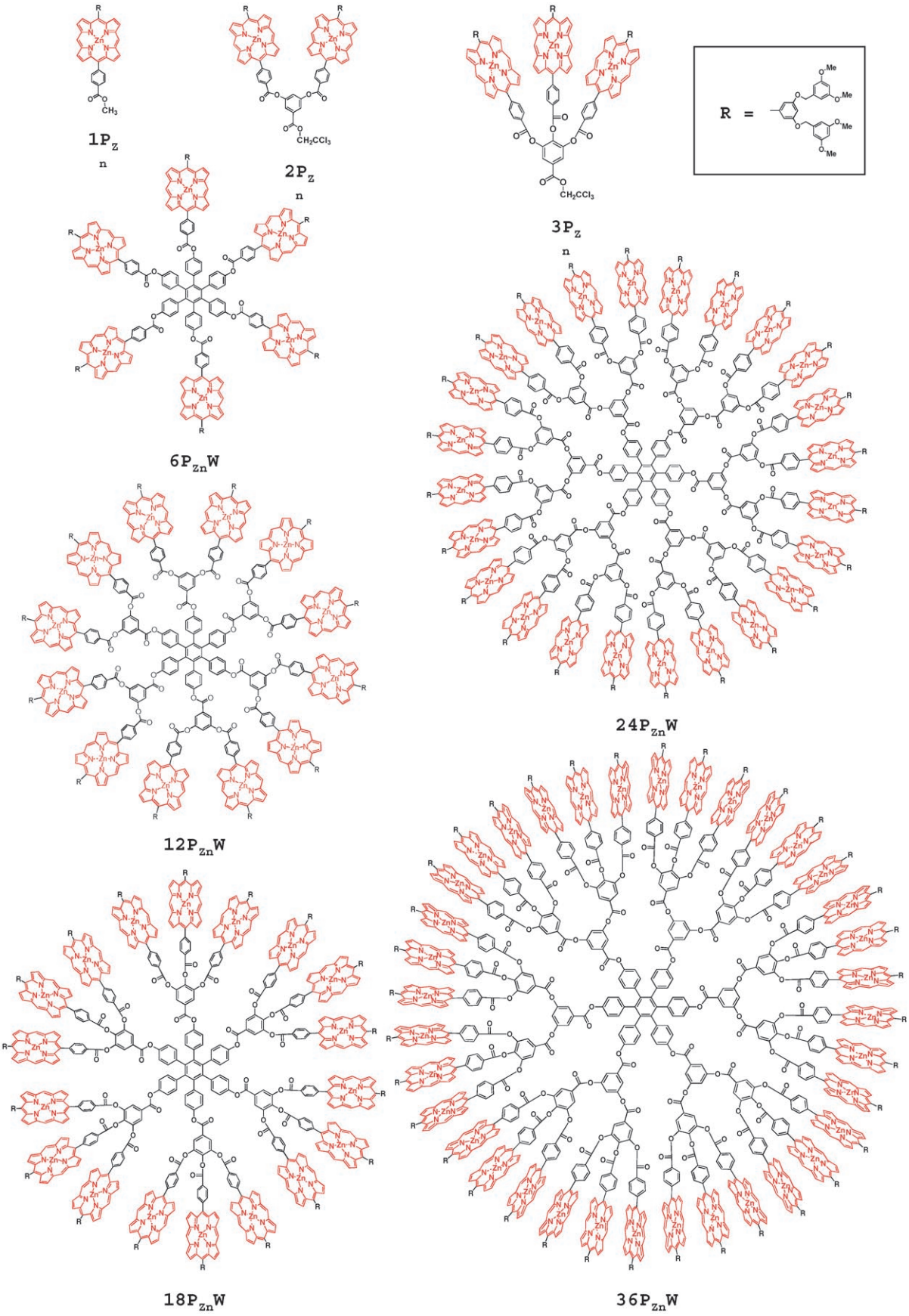

Scheme 1. Structures of zinc(II) porphyrin dendrimers and dendrons.

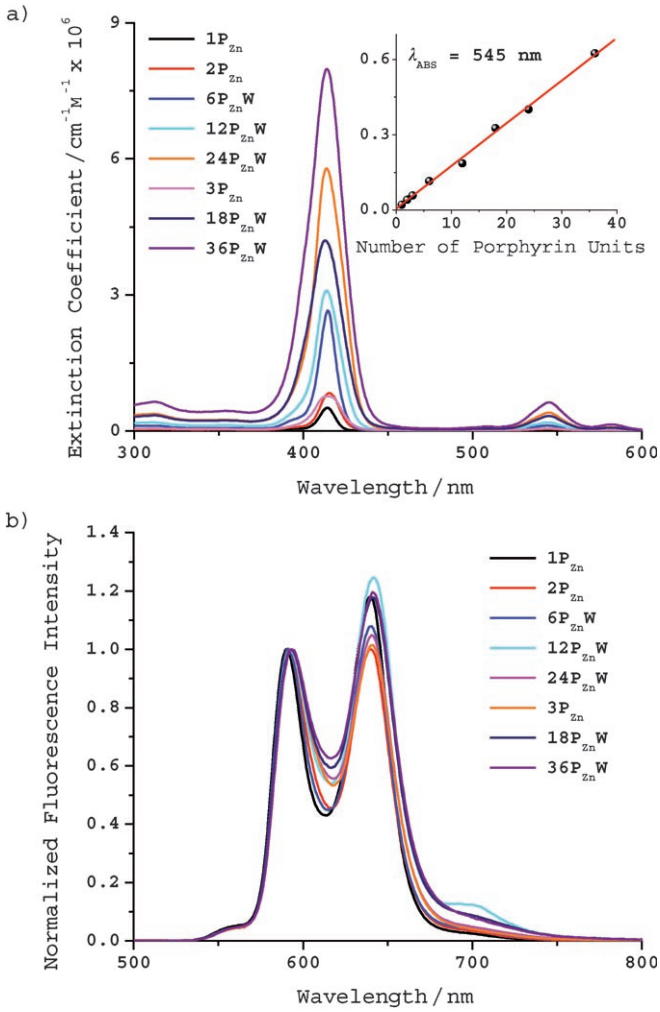

Figure 1. Steady-state absorption (a) and fluorescence (b) spectra of zinc(II) porphyrin dendrimers and dendrons in THF. Inset: plot of extinction coefficient at 545 nm versus number of porphyrin units.

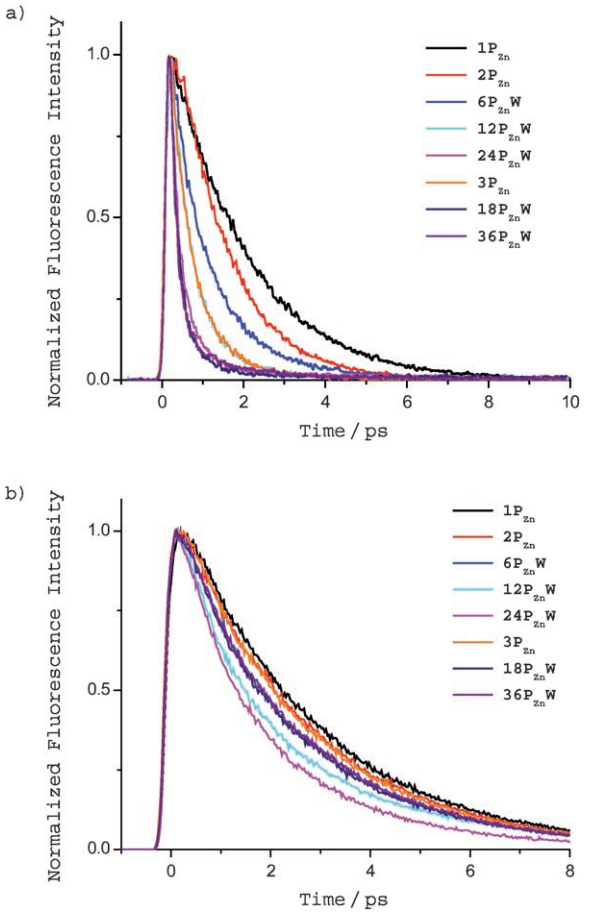

Figure 2. Fluorescence temporal decay profiles of zinc(II) porphyrin dendrimers and dendrons in THF after photoexcitation at 405 nm. a) B band and b) Q-band fluorescence decays at 450 and 650 nm, respectively. See Table 1 for details.

those of dendrons presumably originate from the shielding effect of zinc(II) porphyrin moieties in dendrimers[15] despite the shorter fluorescence lifetimes of zinc(II) porphyrin dendrimers (Table 1). In other words, although **$12P_{Zn}W$** and **$24P_{Zn}W$** dendrimers show fast components in fluorescence decay profiles due to excimer formation, the slow components contributed by the decay of excimer emission compensates the overall fluorescence quantum yields of zinc(II) porphyrin dendrimers (Figure 2b).

Anisotropy decay profiles: Measurements of fluorescence anisotropy decay provide information on rotational diffusion motion and the dynamics of inter- and intrachromophore EET processes. Especially when an initial excitation is transferred to another state whose transition dipole moment is different in direction from that of the initial state, the anisotropy value decays in accordance with the energy-transfer rate. Therefore, time-resolved anisotropy measurement in a multichromophore system is useful for revealing the EET processes. Rotational diffusion times of dendrimers and dendrons in THF were measured by time-correlated single-photon counting (TCSPC) method, because these processes are believed to occur on much slower timescales than EET processes due to the large hydrodynamic molecular volumes of dendrimers and dendrons (Figure 3). As the number of

Table 1. Fitted S_2 and S_1 state fluorescence lifetimes and S_1 state fluorescence quantum yields of zinc(II) porphyrin dendrimers and dendrons in THF.

	Fitted fluorescence lifetime		Φ_F (S_1)[a]
	$\tau(S_2)$ [fs]	$\tau(S_1)$ [ns]	
$1P_{Zn}$	1904	2.41	0.034
$6P_{Zn}W$	983[b]	2.02[b]	0.041
$2P_{Zn}$	1235	2.23	0.036
$12P_{Zn}W$	600[b]	1.81[b]	0.038
$24P_{Zn}W$	402[b]	1.45[b]	0.038
3PZn	583[b]	2.22[b]	0.036
$18P_{Zn}W$	445[b]	1.92[b]	0.029
$36P_{Zn}W$	619[b]	1.96[b]	0.032

[a] Estimated by using zinc(II) tetraphenylporphyrin in toluene as standard (0.033). [b] Weighted average lifetime for a three-exponential fit of the form $A_1\exp[-t/\tau_1]+A_2\exp[-t/\tau_2]+A_3\exp[-t/\tau_3]$.

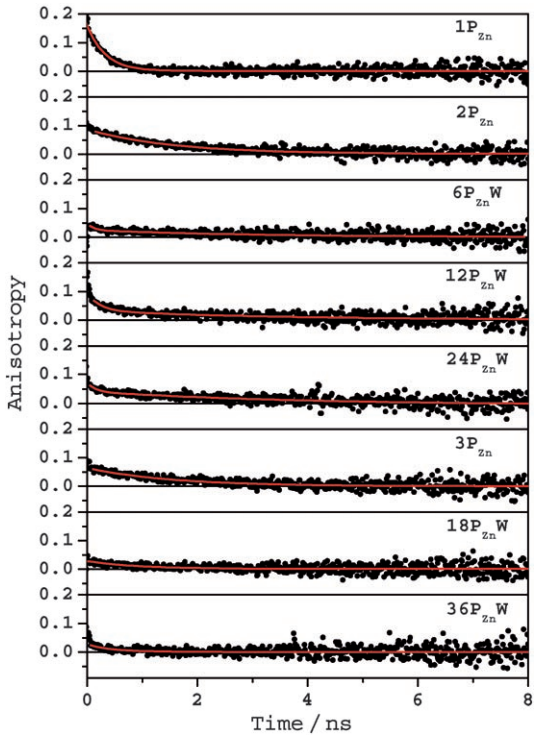

Figure 3. Anisotropy decay profiles of Q-band fluorescence at 650 nm following 405 nm photoexcitation of zinc(II) porphyrin dendrimers and dendrons in THF. See Table 2 for details.

porphyrin units increases, the rotational diffusion time increases and the initial anisotropy value decreases because of EET processes. Two-branched type dendrimers **12P$_{Zn}$W** and **24P$_{Zn}$W** exhibit a saturated rotational time constant of 3.7 ns, that is, the hydrodynamic volume is not proportional to the number of porphyrin units, and consequently the packing efficiency of zinc(II) porphyrin units is high, especially in **24P$_{Zn}$W**. On the other hand, in three-branched type dendrimers **18P$_{Zn}$W** and **36P$_{Zn}$W**, we could not observe the rotational diffusion times, presumably due to their much enlarged hydrodynamic volumes as well as low initial anisotropy values.

To measure the fluorescence anisotropy changes induced by the EET processes in the Q states of dendrimers, we carried out fluorescence up-conversion experiments for better time resolution than the TCSPC method. Accordingly, we measured the fluorescence anisotropy decay at 650 nm following photoexcitation at 550 nm. The initial anisotropy values of dendrimers and dendrons start from a value of about 0.15, similar to that of **1P$_{Zn}$**. The degeneracy of the Q state of zinc(II) porphyrin complicates analysis of the anisotropy decay considerably. Electronic dephasing and intramolecular energy equilibration between the degenerate Q_x and Q_y states can occur prior to the EET process between porphyrin units. For a degenerate system with mutually orthogonal transition dipole moments, as in the Q state of porphyrin, Wynne et al. showed that time-dependent anisotropy $r(t)$ is given as Equations (1) and (2)[16]

$$r(t) = \frac{1}{10}[1 + 3\,e^{-\gamma t} + 3f(t)] \quad (1)$$

$$f(t) = \left[\frac{\gamma/2-\Gamma}{\Omega}\sin(\Omega t) + \cos(\Omega t)\right]e^{-(\gamma/2+\Gamma)t} \quad (2)$$

where $\Omega^2 \equiv b^2 - a^2$, $a \equiv \Gamma + \gamma/2$, $b \equiv \sqrt{4\beta^2 + 2\gamma\Gamma}$, γ is an electronic coherent dephasing decay caused by the energy fluctuations, Γ a decay associated with the coupling fluctuations, and β a coupling between the degenerate states. According to these equations, the anisotropy should exhibit an initial value of 0.7, larger than the normally observed value of 0.4, before electronic dephasing sets in. Then it decays to a value of 0.4, mainly due to electronic dephasing between the two degenerate states. When the two states are completely dephased with equal population, the anisotropy attains a value of 0.1.[17]

In the present case, our interest is focused on the incoherent EET processes occurring in the equilibrated Q states of zinc(II) porphyrin dendrimers. Therefore, according to Equations (1) and (2), the initial anisotropy value of zinc(II) porphyrin unit **1P$_{Zn}$** should start from 0.1 in our experimental time window. However, the transition dipole moment in **1P$_{Zn}$** along the axis of the substituted phenyl ring is larger and energetically lower than that of the other perpendicular axis. As a result, the initial anisotropy value of **1P$_{Zn}$** exhibits a slightly larger value of 0.15. The infinite anisotropy values are inversely proportional to the number of porphyrin units, which is consistent with efficient EET processes in dendrimers. The fast depolarization components which are shorter than the lifetime of the S_1 state seem to originate from the EET processes between the neighboring chromophores in dendrimers. We found two major components: 20–30 ps and 180–280 ps. Unfortunately, we could not retrieve the decay time constants accurately because the signal/noise (S/N) ratio of femtosecond fluorescence up-conversion anisotropy decay was poor. To overcome the low S/N ratio, we measured femtosecond transient absorption anisotropy in dendrimers and dendrons by photoexcitation at 550 nm and probing at 500 nm (Figure 4). Anisotropy data are summarized in Table 2.

Calculation of molecular structures: To analyze the spectroscopic data quantitatively, we calculated the molecular structure by using the semi-empirical AM1 Hamiltonian and found that the overall structures of dendrimers are governed by the rigid hexaarylbenzene core and the steric hindrance of zinc(II) porphyrin units. The most stable geometry of dendrimers has the constituent zinc(II) porphyrin units farthest away from each other. At the same time, however, the rigid core restricts the freedom of zinc(II) porphyrin units to give rise to well-ordered structures.

Geometrically optimized two-branched type dendron **2P$_{Zn}$** has many conformers because of the flexible linkage and enough space to move freely, as evidenced by the broad B band compared with **1P$_{Zn}$** in the steady-state absorption spectrum. Since the energy difference between the calculat-

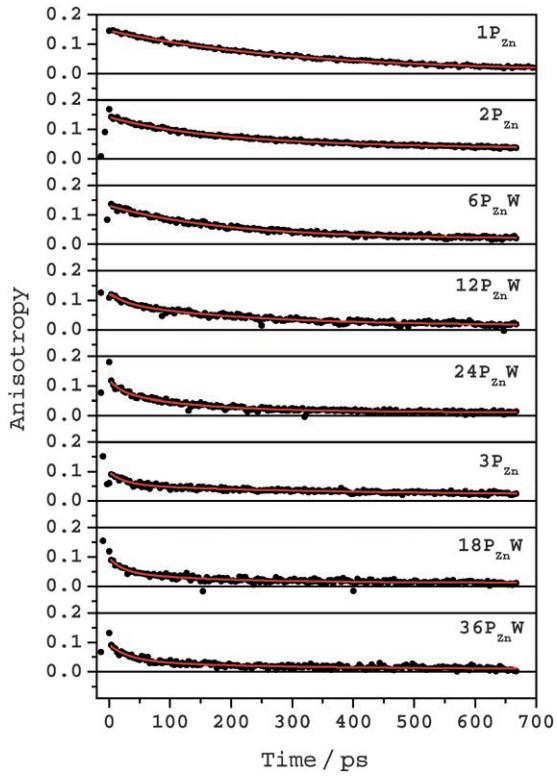

Figure 4. Anisotropy decay profiles of Q-band induced absorption following 550 nm photoexcitation and 500 nm probing by the transient absorption technique of zinc(II) porphyrin dendrimers and dendrons in THF. See Table 2 for details.

Table 2. Fitted anisotropy decay parameters of zinc(II) porphyrin dendrimers and dendrons.

	Anisotropy decay parameters				
	Up-conversion		Transient absorption		Rotational diffusion
	τ_1 [ps]	τ_2 [ps]	τ_1 [ps]	τ_2 [ps]	τ_3 [ns]
$1P_{Zn}$					0.32 ± 0.01
$6P_{Zn}W$		190 ± 2		180.7 ± 0.2	2.98 ± 0.14
$2P_{Zn}$		180 ± 4		158.2 ± 0.6	1.60 ± 0.10
$12P_{Zn}W$	27 ± 5	218 ± 7	24.2 ± 0.6	207.8 ± 5.0	3.34 ± 0.39
$24P_{Zn}W$	26 ± 5	172 ± 11	18.9 ± 0.1	130.7 ± 2.2	3.69 ± 0.86
$3P_{Zn}$	32 ± 5	287 ± 23	26 ± 0.3	211.5 ± 4.8	1.56 ± 0.14
$18P_{Zn}W$	30 ± 9	181 ± 48	21.9 ± 0.7	137.7 ± 7.5	0.90 ± 0.17[a]
$36P_{Zn}W$	16 ± 5	200 ± 91	33.1 ± 0.9	205.0 ± 9.0	0.74 ± 0.55[a]

[a] This time constant is not due to the rotational diffusion motion but to the EET processes (see text).

ed conformers of **$2P_{Zn}$** is smaller than thermal energy (kT), the conformers of **$2P_{Zn}$** are in thermal equilibrium (see Supporting Information). On the contrary, geometry optimized three-branched type dendron **$3P_{Zn}$** has only a few conformers because of steric hindrance of zinc(II) porphyrin units resulting in a triangular arrangement (see Supporting Information). The calculated molecular structure of **$6P_{Zn}W$** exhibits a well-ordered two-dimensional hexagonal shape induced by the rigid core in which all six porphyrin units are in one plane to form a large wheel (Scheme 2). On the other hand, the optimized structure of **$12P_{Zn}W$** shows a zigzag up-and-down three-dimensional structure in which six porphyrin units are located above the core plane and the other six below it (Scheme 2). The structures of **$24P_{Zn}W$**, **$18P_{Zn}W$**, and **$36P_{Zn}W$** could not be optimized because of their large molecular size.

Discussion

Assuming that the interchromophore interactions are weak, we could calculate the EET rates of dendrimers based on the depolarization time constants by using the interchromophore distance and orientation factor in the optimized geometry. The EET process is assumed to occur only between neighboring porphyrin units. Since the timescales of the EET processes of dendrimers are on the order of a few hundred picoseconds, the overall rotational diffusion can be discriminated in anisotropy decay because it is at least on the order of a few nanoseconds. Nevertheless, we have to consider the origin of fast depolarization processes, because both EET process and local rotational motion could affect the fast depolarization dynamics. However, the local rotational motions in dendrimers and dendrons should involve the rotational axis which is along the direction of the substituted phenyl ring due to the dendron structures. Therefore, although local rotational motions in dendrimers and dendrons occur, the direction of the dipole moment along the substituted phenyl ring in the zinc(II) porphyrin moiety does not change. Thus, we can expect that local rotation motions do not make a significant contribution to changes in depolarization. Moreover, dendrimers exhibit three-dimensionally packed structures which prohibit local rotational motion. Consequently, we can conclude that the contribution to the depolarization dynamics by local rotational motions in dendrimers and dendrons are negligible.

One-branched type dendron **$1P_{Zn}$** exhibits a single anisotropy decay component corresponding to a rotational diffusion time of (320 ± 10) ps. On the other hand, one-branched type dendrimer **$6P_{Zn}W$** shows mono-exponential anisotropy decay (Figure 4) from which an EET time constant of (542 ± 1) ps ($k_{dep}=3k_{hop}$) between the zinc(II) porphyrin units could be derived from the optimized hexagonal structure. This result is in a good accordance with the value of 487 ps calculated by the AM1 Hamiltonian on the basis of the molecular geometry, and this shows that the porphyrin units are located in-plane with a well-ordered two-dimensional circular geometry (see Supporting Information). Two-branched type dendron **$2P_{Zn}$** shows a fast EET time constant of (316 ± 2) ps ($k_{dep}=2k_{hop}$) compared with the value of 1551 ps calculated by using the average interchromophore distance and randomized orientation factor ($\kappa^2=2/3$). How-

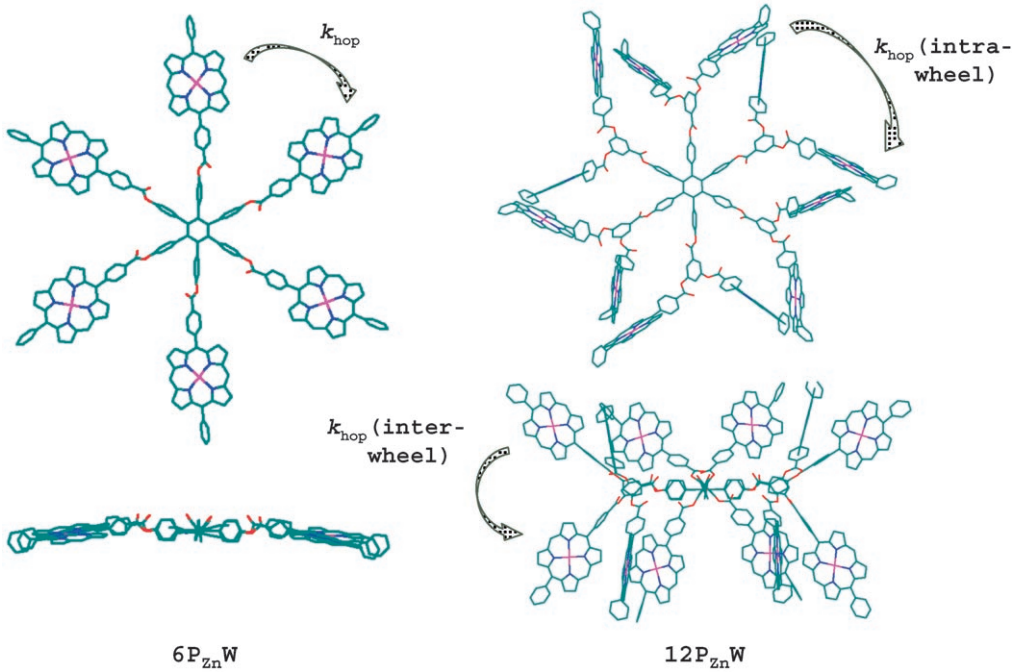

Scheme 2. Incoherent energy-migration processes in zinc(II) porphyrin dendrimers; **$6P_{Zn}W$** and **$12P_{Zn}W$**.

ever, the calculated energy-migration time for conformer **$2P_{Zn}$** with a short interchromophore distance matches well with the experimental result. Accordingly, the discrepancy between experimental and theoretical results of **$2P_{Zn}$** is presumably attributable to conformers with long interchromophore distance between zinc(II) porphyrin units, because the EET process strongly depends on the interchromophore distance (see Supporting Information). Two-branched type dendrimer **$12P_{Zn}W$** shows biexponential anisotropy decay (Figure 4). The structure of **$12P_{Zn}W$** optimized by the AM1 Hamiltonian suggests dual hexagonal wheels in a staggered conformation (Scheme 2). Thus the fast anisotropy decay is attributable to interwheel and the slow component to intrawheel EET processes, because the optimized interchromophore distance is shorter between neighboring porphyrins residing on different wheels than that in the same hexagonal wheel. The experimental EET times between the porphyrin units in **$12P_{Zn}W$** are (24 ± 1) ps (interwheel, $k_{dep}=k_{interwheel}$) and (623 ± 15) ps (intrawheel, $k_{dep}=3k_{intrawheel}$). Two-branched type dendrimer **$24P_{Zn}W$** also shows biexponential anisotropy decay, which is faster than that of **$12P_{Zn}W$** (Figure 4). From the similar rotational diffusion time of **$24P_{Zn}W$** to that of **$12P_{Zn}W$**, it is thought that the hydrodynamic volume of **$24P_{Zn}W$** does not increase significantly as the number of porphyrin units increases. Therefore, we could expect that the porphyrin units are tightly packed and form a congested wheel structure in **$24P_{Zn}W$**, which leads to faster energy migration processes because of short interchromophore distances. However, since the molecular geometry of **$24P_{Zn}W$** could not be optimized exactly because of its large molecular size, we could not derive the EET times from the anisotropy depolarization times. Assuming that **$24P_{Zn}W$** is composed of two **$12P_{Zn}W$** dendrimers with twin-wheel structures, we can suggest that fast and slow depolarization changes arise from the inter- and intrawheel EET processes, respectively, because of the similarities in structures between **$12P_{Zn}W$** and **$24P_{Zn}W$**.

In contrast with **$2P_{Zn}$**, three-branched type dendron **$3P_{Zn}$** exhibits biexponential anisotropy decay indicating dual energy-migration paths between porphyrin units (see Supporting Information). The fast and slow anisotropy decay components could be assigned to the energy-migration times between neighboring porphyrins and between the next nearest neighbor porphyrins, respectively, in **$3P_{Zn}$**. The similarity of the rotational diffusion time of **$3P_{Zn}$** to that of **$2P_{Zn}$** indicates that **$3P_{Zn}$** forms a compact three-dimensional triangular structure. Three-branched type dendrimers **$18P_{Zn}W$** and **$36P_{Zn}W$** exhibit biexponential anisotropy decays with similar time constants to those of their constituent units **$3P_{Zn}$**. This feature suggests that the **$3P_{Zn}$** constituent unit acts as a cluster in the EET processes in **$18P_{Zn}W$** and **$36P_{Zn}W$**. The slow depolarization times of 900 and 740 ps detected by the TCSPC method could be assigned to intercluster energy-migration processes in **$18P_{Zn}W$** and **$36P_{Zn}W$**, respectively. Thus, although geometry optimized structures of **$18P_{Zn}W$** and **$36P_{Zn}W$** dendrimers are not available, we could suggest that the cluster units of **$3P_{Zn}$** are located as far from each other as possible in three-dimensional space in dendrimers **$18P_{Zn}W$** and **$36P_{Zn}W$** based on the observed depolarization time constants. The calculated energy-migration times based on the Förster-type EET model (see Supporting Information) follow: 1551 ps (**$2P_{Zn}$**), 71 and 653 ps (**$3P_{Zn}$**), 487 ps (**$6P_{Zn}W$**), and 59 and 622 ps (**$12P_{Zn}W$**). Accordingly, the experimental depolarization and EET times in dendrimers are

well matched with theoretical model of through-space energy migration induced by dipole–dipole interactions between zinc(II) porphyrin units.

Conclusion

The photophysical properties of hexaarylbenzene-anchored polyester zinc(II) porphyrin dendrimers strongly depend on the molecular structures, which are determined by the rigidity of cores and the types of dendrons. Tightly packed three-dimensional structures of dendrimers enhance the efficiency of EET processes between the constituent chromophore units and lead to effective artificial light-harvesting system compared with other types of molecular assembles. In contrast with the two-dimensional EET process in one-branched type dendrimer **6P$_{Zn}$W**, two-branched type dendrimers **12P$_{Zn}$W** and **24P$_{Zn}$W** exhibit tightly packed geometries with staggered multilayer hexagonal-wheel structures that lead to fast three-dimensional EET processes between the hexagonal wheels. As a result, there are two main EET paths in dendrimers; interwheel (fast) and intrawheel (slow) energy-migration processes. On the other hand, three-branched type dendrimers show that the **3P$_{Zn}$** constituent unit acts as a cluster in the EET processes of **18P$_{Zn}$W** and **36P$_{Zn}$W** because the porphyrin units in **3P$_{Zn}$** are already in close contact. Therefore, we suggest that fast EET processes occur in a cluster and then slow EET processes between the clusters. Thus, we can propose that three-dimensional dendrimer structures and EET processes are strongly associated with each other. Finally, two-branched type dendrimers with congested, well-ordered, and tightly packed structures could be promising systems for mimicking the oxygenic light-harvesting complex in view of their three-dimensionally ordered geometries, enormous absorbing capacity, efficient multipath EET processes, and synthetic simplicity.

Experimental Section

Sample preparation: The zinc(II) porphyrin dendrimers and dendrons were synthesized according to literature methods.[14] The THF (~99.8% purity) used as solvent was purchased from Merck Chemical Co. (HPLC grade) and used without further purification. All measurements were performed at ambient temperature (22±1°C).

Steady-state absorption and fluorescence: Absorption spectra were obtained with a Shimadzu model 1601 UV spectrometer, and steady-state fluorescence and excitation spectra were measured by a Hitachi model F-2500 fluorometer at room temperature. The fluorescence quantum yield was obtained by comparison to the fluorescence quantum yield of about 0.03 of a zinc(II) 5,15-diphenylporphine in THF at ambient temperature (22±1°C).

TCSPC measurements: A time-correlated single-photon counting (TCSPC) system was used for measurements of spontaneous fluorescence decay and fluorescence anisotropy decay. The system consisted of a cavity-dumped Kerr lens mode-locked Ti:sapphire laser pumped by a continuous-wave Nd:YVO_4 laser (Coherent, Verdi). The full width at half maximum (FWHM) of the instrument response function (IRF) obtained by a dilute solution of coffee cream was typically 70 ps in our TCSPC system. The fluorescence decays were measured with magic-angle (54.7°) fluorescence polarization, and the number of fluorescence photons per unit time, detected by a photomultiplier tube, was always maintained at <1% of the repetition rate of the excitation pulses to prevent pile-up distortion in the decay profiles. The intensity of excitation pulses was carefully controlled by a variable neutral density filter to prevent multiphoton processes such as singlet–singlet annihilation. Time-resolved fluorescence anisotropy decays were obtained by changing the detection polarization on the fluorescence path to parallel or perpendicular to the polarization of the excitation pulses. The anisotropy decay then was calculated from Equation (3)

$$r(t) = \frac{I_{VV}(t) - GI_{VH}(t)}{I_{VV}(t) + 2GI_{VH}(t)} \quad (3)$$

where $I_{VV}(t)$ [or $I_{VH}(t)$] is the fluorescence decay when the excitation light is vertically polarized and only the vertical (or horizontally) polarized portion of fluorescence is detected, and the first and second subscripts represent excitation and detection polarization, respectively. The factor G is defined by $I_{VV}(t)/I_{VH}(t)$, which is equal to the ratio of the sensitivities of the detection system for vertical and horizontal polarization. The G factor of our system was 1.08.

Femtosecond fluorescence up-conversion measurement and anisotropy measurement pumped by IR OPO: A femtosecond fluorescence up-conversion apparatus was used for the time-resolved spontaneous fluorescence. The beam sources for the B- and Q state fluorescence were a home-built cavity-dumped Kerr lens mode-locked Ti:sapphire oscillator[18] and a cavity-dumped near-infrared optical parametric oscillator[19] tunable in the near-infrared region, respectively. The second harmonic of the fundamental generated in a 100-μm thick β-barium borate (BBO) crystal served as pump pulse. Residual fundamental pulse was used as a gate pulse. Three pairs of fused silica Brewster angle prisms compensate group-velocity dispersions of the fundamental pulse prior to second harmonic generation, the second harmonic around 400 and 550 nm, and the residual fundamental pulses. The pump beam was focused onto a 500-μm thick cuvette containing sample solution by a lens with 5-cm focal length. The cuvette was mounted on a motor-driven stage and moved constantly back and forth to minimize photodamage. Collection of the fluorescence and focusing into a BBO crystal for frequency conversion was achieved by a reflecting microscope objective lens. A 500-μm thick BBO crystal was used for up-conversion of the B band fluorescence. The FWHMs of the cross-correlation function between the scattered pump pulse and the gate pulse were 80 and 120 fs, respectively. For the anisotropy measurements, I_{VV} and I_{VH} were recorded to obtain the anisotropy by using Equation (4)

$$r(t) = \frac{I_{VV}(t) - GI_{VH}(t)}{I_{VV}(t) + 2GI_{VH}(t)} \quad (4)$$

where I_{VV} and I_{VH} represent up-converted signals with polarization of excitation and fluorescence vertically and horizontally polarized, respectively. The correction factor G was obtained by tail matching fluorescence (I_{VV} and I_{VH}) for a rhodamine dye at long times.

Femtosecond transient absorption anisotropy: The femtosecond time-resolved transient absorption anisotropy apparatus consisted of home-built visible dual noncollinear optical parametric amplifiers (NOPAs) pumped by a Ti:sapphire regenerative amplifier laser (Spectra Physics, Hurricane) and an optical detection system. The output beam from the Hurricane had a pulse width of about 130 fs and a power of about 1 W at a repetition rate of 5 kHz, which was divided into two parts by a 1:1 beam splitter. Each beam was color-tuned for the pump and probe beams by a NOPA. The resulting laser pulses had a temporal width of about 30 fs in the visible range (500–700 nm). The pump and probe beams were focused and overlapped at the sample position. The time delay between pump and probe beams was controlled by making the pump beam travel along a variable optical delay line. The intensities of pump and probe beams were monitored by a reference photodiode compensating the experimental data. The probe beam was split by a cubic polarizer into relative polarizations parallel and perpendicular to that of pump beam. The polar-

ized probe beams were recorded by dual photodiodes. Finally, the transient absorption anisotropy decay was obtained by Equation (5)

$$r(t) = \frac{\Delta A_{VV}(t) - \Delta A_{HV}(t)}{\Delta A_{VV}(t) - 2\,\Delta A_{HV}(t)} \quad (5)$$

where $\Delta A_{VV}(t)$ [or $\Delta A_{VH}(t)$] is the absorbance change when the pump beam is vertically polarized and only the vertically (or horizontally) polarized portion of absorbance change is detected, and the first and second subscripts represent excitation and detection polarization, respectively.

Acknowledgements

This research was financially supported by the National Creative Research Initiatives Program of the Korea Science and Engineering Foundation of Korea (D.K.). The work at Tokyo was supported by Exploratory Research for Advanced Technology (ERATO), Japan Science and Technology Agency (JST). We thank Dr. H. Rhee and Prof. T. Joo at POSTECH for OPO up-conversion experiments.

[1] P. Jordan, P. Fromme, H. T. Witt, O. Klukas, W. Saenger, N. Krauß, *Nature* **2001**, *411*, 909.
[2] a) A. M. van Oijen, M. Ketelaars, J. Köhler, T. J. Aartsma, J. Schmidt, *Science* **1999**, *285*, 400; b) T. Polivka, V. Sundström, *Chem. Rev.* **2004**, *104*, 2021.
[3] a) S. E. Bradforth, R. Jimenez, F. van Mourik, R. van Grondelle, G. R. Fleming, *J. Phys. Chem.* **1995**, *99*, 16179; b) R. Jimenez, S. N. Dikshit, S. E. Bradforth, G. R. Fleming, *J. Phys. Chem.* **1996**, *100*, 6825.
[4] D. Holten, D. F. Bocian, J. S. Lindsey, *Acc. Chem. Res.* **2002**, *35*, 57.
[5] M. R. Wasielewski, *Chem. Rev.* **1992**, *92*, 435.
[6] a) D. Kim, A. Osuka, *J. Phys. Chem. A* **2003**, *107*, 8791; b) D. Kim, A. Osuka, *Acc. Chem. Res.* **2004**, *37*, 735; c) H. S. Cho, D. H. Jeong, S. Cho, D. Kim, Y. Mastuzaki, Tanaka, A. K. Tsuda, A. Osuka, *J. Am. Chem. Soc.* **2002**, *124*, 14642; d) N. Aratani, H. S. Cho, T. K. Ahn, S. Cho, D. Kim, H. Sumi, A. Osuka, *J. Am. Chem. Soc.* **2003**, *125*, 9668.
[7] H. S. Cho, H. Rhee, J. K. Song, C.-K. Min, M. Takase, N. Aratani, S. Cho, A. Osuka, D. Kim, *J. Am. Chem. Soc.* **2003**, *125*, 5849.
[8] a) M.-S. Choi, T. Yamazaki, I. Yamazaki, T. Aida, *Angew. Chem.* **2004**, *116*, 152; *Angew. Chem. Int. Ed.* **2004**, *43*, 150; b) M.-S. Choi, T. Aida, T. Yamazaki, I. Yamazaki, *Chem. Eur. J.* **2002**, *8*, 2668; c) M.-S. Choi, T. Aida, H. Luo, Y. Araki, O. Ito, *Angew. Chem.* **2003**, *115*, 4194; *Angew. Chem. Int. Ed.* **2003**, *42*, 4060.
[9] a) E. K. L. Yeow, K. P. Ghiggino, J. N. Reek, M. J. Crossley, A. W. Bosman, A. P. H. J. Schenning, E. W. Meijer, *J. Phys. Chem. B* **2000**, *104*, 2596; b) J. Larsen, J. Andersson, T. Polivka, J. Sly, M. J. Crossley, V. Sundströom, E. Åkesson, *Chem. Phys. Lett.* **2005**, *403*, 205.
[10] a) I.-W. Hwang, T. Kamada, T. K. Ahn, D. M. Ko, T. Nakamura, A. Tsuda, A. Osuka, D. Kim, *J. Am. Chem. Soc.* **2004**, *126*, 16187; b) R. Takahashi, Y. Kobuke, *J. Org. Chem.* **2005**, *70*, 2745; c) X. Peng, N. Aratani, A. Takagi, T. Matsumoto, T. Kawai, I.-W. Hwang, T. K. Ahn, D. Kim, A. Osuka, *J. Am. Chem. Soc.* **2004**, *126*, 4468; d) I.-W. Hwang, M. Park, T. K. Ahn, Z. S. Yoon, D. M. Ko, D. Kim, F. Ito, Y. Ishibashi, S. R. Khan, Y. Nagasawa, H. Miyasaka, C. Ikeda, R. Takahashi, K. Ogawa, A. Satake, Y. Kobuke, *Chem. Eur. J.* **2005**, *11*, 3753.
[11] a) T. Hasobe, P. V. Kamat, M. A. Absalom, Y. Kashiwagi, J. Sly, M. J. Crossley, K. Hosomizu, H. Imahori, S. Fukuzumi, *J. Phys. Chem. B* **2004**, *108*, 12865; b) M. Ayabe, A. Ikeda, Y. Kubo, M. Takeuchi, S. Shinkai, *Angew. Chem.* **2002**, *114*, 2914; *Angew. Chem. Int. Ed.* **2002**, *41*, 2790.
[12] a) O. P. Varnavski, J. C. Ostrowski, L. Sukhomlinova, R. J. Twieg, G. C. Bazan, T. Goodson III. , *J. Am. Chem. Soc.* **2002**, *124*, 1736; b) D. A. Tomalia, A. M. Naylor, W. A. Goddard III, *Angew. Chem.* **1990**, *102*, 119; *Angew. Chem. Int. Ed. Engl.* **1990**, *29*, 138.
[13] a) J. Hofkens, L. Latterini, G. De Belder, T. Gensch, M. Maus, T. Vosch, Y. Karni, G. Schweitzer, F. C. De Schryver, *Chem. Phys. Lett.* **1999**, *304*, 1; b) M. Maus, R. De, M. Lor, T. Weil, S. Mitra, U.-M. Wiesler, A. Herrmann, J. Hofkens, T. Vosch, K. Mullen, F. C. De Schryver, *J. Am. Chem. Soc.* **2001**, *123*, 7668.
[14] W.-S. Li, D.-L. Jiang, Y. Suna, T. Aida, *J. Am. Chem. Soc.* **2005**, *127*, 7700.
[15] S. Hecht, H. Ihre, J. M. J. Frechet, *J. Am. Chem. Soc.* **1999**, *121*, 9239.
[16] a) K. Wynne, R. M. Hochstrasser, *Chem. Phys.* **1993**, *171*, 179; b) K. Wynne, R. M. Hochstrasser, *J. Raman Spectrosc.* **1995**, *26*, 561.
[17] a) C. Galli, K. Wynne, S. M. Lecours, M. J. Therien, R. M. Hochstrasser, *Chem. Phys. Lett.* **1994**, *100*, 6672; b) K. Wynne, S. M. Lecours, C. Galli, M. J. Therien, R. M. Hochstrasser, *J. Am. Chem. Soc.* **1995**, *117*, 3749.
[18] M.-C. Yoon, D. H. Jeong, S. Cho, D. Kim, H. Rhee, T. Joo, *J. Chem. Phys.* **2003**, *118*, 164.
[19] C.-K. Min, T. Joo, *Opt. Lett.* **2005**, *30*, 1855.

Received: February 15, 2006
Revised: April 27, 2006
Published online: July 6, 2006

